

REPORTS

hemoglobin variant that confers protection against malaria primarily to individuals homozygous for the C allele (37). This is consistent with the assertion by Modiano and co-workers that the ideal epidemiological context for selection of such a protective genetic factor is one with very high rates of malaria transmission (37). The selection among human populations of other genetic traits protective against malaria appears also to be consistent with the above entomological inference because it offers good evidence that mortality due to *P. falciparum* has been common only within the past 6000 years or less (38, 39). The tremendous rise in malaria transmission that accompanied the speciation of *A. gambiae* may have influenced the emergence of modern *P. falciparum* from a less pathogenic, ancestral parasite (27). The large increase in the rate of parasite transmission could have favored the selection of fast-growing, aggressive strains responsible for acute, short-lived infections. Such recent emergence of the pathogenic *P. falciparum* is supported by at least some of the genetic studies on the parasite (40, 41).

The availability of the complete *A. gambiae* genome will greatly accelerate study of the evolution of this complex taxon and its siblings. The close linkage between the genome sequence and the polytene chromosome complement (42) is already being used to analyze sequences at the breakpoints of major polymorphic inversions, particularly those that are diagnostic for chromosomal forms. Molecular assays for these inversions will allow analysis of the population genetics and ecology of chromosomal forms to be extended to all life stages, including early instar larvae and adult males in which polytene chromosomes cannot be analyzed directly. However, it will almost certainly be analysis of sets of alleles balanced by inversions covering genes in the central area of 2R that will be among the most important and rewarding challenges for post genomic study of *A. gambiae* and its siblings.

References and Notes

1. The name *Anopheles gambiae* alone, i.e., not followed by the word "complex," is used throughout the text to refer to the nominotypical species *Anopheles gambiae* Giles, 1902, *sensu stricto*.
2. G. Davidson, *Riv. Malariol.* **43**, 167 (1964).
3. M. Coluzzi, *Rend. Acc. Naz. Lincei* **40**, 671 (1966).
4. ———, A. Sabatini, *Parassitologia* **9**, 73 (1967).
5. ———, *Parassitologia* **10**, 155 (1968).
6. ———, *Parassitologia* **11**, 177 (1969).
7. M. Coluzzi *et al.*, *Trans. R. Soc. Trop. Med. Hyg.* **73**, 483 (1979).
8. M. Coluzzi *et al.*, unpublished observations.
9. J. H. Bryan *et al.*, *Parassitologia* **29**, 221 (1987).
10. V. Petrarca *et al.*, *Parassitologia* **26**, 247 (1984).
11. V. Petrarca *et al.*, *Med. Vet. Entomol.* **14**, 149 (2000).
12. G. Davidson, C. E. Jackson, *Bull. W.H.O.* **27**, 303 (1962).
13. Y. T. Touré *et al.*, *Genetica* **94**, 213 (1994).
14. A. della Torre *et al.*, *Genetics* **146**, 239 (1997).
15. J. R. Powell *et al.*, *Parassitologia* **41**, 101 (1999).
16. Y. T. Touré, V. Petrarca, M. Coluzzi, *Parassitologia* **25**, 367 (1983).

17. Y. T. Touré *et al.*, *Parassitologia* **40**, 477 (1998).
18. M. Coluzzi, V. Petrarca, M. A. Di Deco, *Boll. Zool.* **52**, 45 (1985).
19. A. della Torre *et al.*, *Science* **298**, 115 (2002).
20. G. Favia *et al.*, *Insect Mol. Biol.* **6**, 377 (1997).
21. A. della Torre *et al.*, *Insect Mol. Biol.* **10**, 9 (2001).
22. C. Fanello *et al.*, *Insect Mol. Biol.*, in press.
23. M. Coluzzi, in *Mechanisms of Speciation*, C. Barigozzi, Ed. (Liss, New York, 1982), pp. 143–153.
24. C. Costantini *et al.*, in preparation.
25. G. B. White, *Trans. R. Soc. Trop. Med. Hyg.* **68**, 278 (1974).
26. F. B. Livingstone, *Am. Anthropol.* **60**, 533 (1958).
27. M. Coluzzi, *Acc. Naz. Lincei Seminario* **23**, 263 (1997).
28. ———, *Parassitologia* **41**, 277 (1999).
29. R. Oslisly, *Azania* **24–25**, 324 (1995).
30. P. Lavachery *et al.*, *Anthropol. Prehist.* **107**, 197 (1996).
31. J. Maley, in *Third Millennium BC Climate Change and Old World Collapse*, H. N. Dalfes, G. Kukla, H. Weiss, Eds. (NATO Adv. Sci. Inst. Series, Global Environmental Change, Springer Verlag, Berlin, 1997), pp. 611–640.
32. J. Maley, *Bull. Inst. Dev. Stud.* (Brighton University) **33**, 13 (2002).
33. M. Coluzzi, *Parasitol. Today* **8**, 113 (1992).
34. C. Garrett-Jones, *Nature* **204**, 1173 (1964).
35. M. Coluzzi, C. Costantini, V. Petrarca, in preparation.
36. L. L. Cavalli-Sforza, P. Menozzi, A. Piazza, Eds., *The History and Geography of Human Genes* (Princeton Univ. Press, Princeton, NJ, 1994), pp. 1–518.
37. D. Modiano *et al.*, *Nature* **414**, 3058 (2001).
38. J. Flint *et al.*, *Bailliere's Clin. Haematol.* **6**, 215 (1993).
39. S. A. Tishkoff *et al.*, *Science* **293**, 455 (2001).
40. S. M. Rich *et al.*, *Proc. Natl. Acad. Sci. U.S.A.* **95**, 4425 (1998).
41. S. K. Volkman *et al.*, *Science* **293**, 482 (2001).
42. R. Holt *et al.*, *Science* **298**, 129 (2002).
43. H. L. Carson, *Am. Nat.* **103**, 323 (1969).
44. R. H. Hunt, M. Coetzee, M. Fette, *Trans. R. Soc. Trop. Med. Hyg.* **92**, 231 (1998).

45. M. Wasserman, *Am. Nat.* **97**, 333 (1963).
46. H. L. Carson, F. E. Clayton, H. D. Stalker, *Proc. Natl. Acad. Sci. U.S.A.* **57**, 1280 (1967).
47. Investigations on the *A. gambiae* complex reviewed in the present paper began in 1964, starting with laboratory material provided by G. Davidson, London School of Hygiene and Tropical Medicine, and continued with analysis of field samples obtained through long-term collaborations between the Malaria Unit of the University of Rome "La Sapienza" (acting as World Health Organization Collaborating Center for Malaria Epidemiology) and many African institutions and collaborators in Benin, Burkina Faso, Ethiopia, Ghana, Guinea Bissau, Ivory Coast, Madagascar, Mali, Mozambique, Nigeria, Senegal, Somalia, Sudan, Tanzania, The Gambia, and Togo. Training and research activities were supported by Control of Tropical Diseases/Malaria (CTD/MAL), WHO, and The U.N. Development Program–World Bank–WHO Special Program for Research and Training in Tropical Diseases (TDR); the Italian Ministry of Foreign Affairs Directorate for Cooperation to Development; the Italian Ministry for Education, University, and Research; the European Union; the Rockefeller Foundation; and the Compagnia di San Paolo. We thank G. Petrangeli for technical assistance and N. Besansky, F. H. Collins, J. R. Powell, G. B. White and two reviewers for useful comments and improvements on the manuscript. Among the African collaborators, we would like to mention particularly the contribution of Y. T. Touré and his team from the Medical School at Bamako, Mali.

Supporting Online Material

www.sciencemag.org/cgi/content/full/1077769/DC1
Materials and Methods
Figs. S1 and S2
Tables S1 to S3

27 August 2002; accepted 25 September 2002
Published online 3 October 2002;
10.1126/science.1077769
Include this information when citing this paper.

On the Origin of Interictal Activity in Human Temporal Lobe Epilepsy in Vitro

Ivan Cohen,¹ Vincent Navarro,^{2,4} Stéphane Clemenceau,^{1,3} Michel Baulac,^{1,2} Richard Miles^{1,*}

The origin and mechanisms of human interictal epileptic discharges remain unclear. Here, we describe a spontaneous, rhythmic activity initiated in the subiculum of slices from patients with temporal lobe epilepsy. Synchronous events were similar to interictal discharges of patient electroencephalograms. They were suppressed by antagonists of either glutamatergic or γ -aminobutyric acid (GABA)–ergic signaling. The network of neurons discharging during population events comprises both subicular interneurons and a subgroup of pyramidal cells. In these pyramidal cells, GABAergic synaptic events reversed at depolarized potentials. Depolarizing GABAergic responses in neurons downstream to the sclerotic CA1 region contribute to human interictal activity.

Mesial temporal lobe epilepsy is the most frequent and severe form of adult focal epilepsy. It is usually refractory to drug therapy and often

associated with sclerosis of the CA1 and CA3 regions of the hippocampus (1). Intracranial electroencephalogram (EEG) records from hippocampal structures usually reveal interictal spikes, lasting 50 to 300 ms, which occur between seizures. Similar activities may be induced in slice or animal models of limbic epilepsy (2–5), but whether they reproduce all aspects of the human pathology remains doubtful (6, 7). One way to resolve this problem is to

¹EMI 0224, CHU Pitié-Salpêtrière, Université Paris VI, 75013 Paris, France. ²Epilepsy Unit, ³Department of Neurosurgery, ⁴CNRS UPR640, Hôpital Pitié-Salpêtrière AP-HP, 75013, Paris, France.

*To whom correspondence should be addressed. E-mail: rmiles@biomedicale.univ-paris5.fr.

REPORTS

study human epileptic tissue that has been removed therapeutically. However, although convulsants initiate epileptiform activity in human tissue, synchronous interictal-like discharges have rarely been observed (8–10).

We carried out this study on specimens from 21 patients with mesial temporal lobe epilepsy (11). In each patient, magnetic resonance imaging revealed a hippocampal atrophy suggestive of sclerosis (12). Scalp or intracranial EEGs showed that seizures originated in the temporal lobe. Unilateral resection of part of this structure, including the hippocampal formation, was indicated because seizures were poorly controlled by antiepileptic drugs (13).

In slices prepared from this tissue (14), the size of both CA1 and CA3 regions was reduced and a laminar organization of pyramidal cell bodies was hard to detect (Fig. 1A). We recorded neuronal activity with intracellular electrodes and extracellular tungsten electrodes, which detect firing of neurons located within a radius of about 100 μm (15). Spontaneous activity was rarely evident in the CA3 or CA1 regions or in the dentate gyrus (Fig. 1, B and C). However, we always detected large extracellular spikes in records from the subiculum, an output region of the hippocampus projecting to the temporal cortex and normally innervated by CA1 pyramidal cell axons (16). In all 31 slices examined, barrages of unit spikes occurred rhythmically and synchronously in records from subicular sites separated by distances of up to 5 mm (Fig. 1, B and C). Synchronous activity was maintained for 8 to 12 hours and persisted when the subiculum was isolated ($n = 15$), showing that it was generated within this structure (Fig. 1D). The timing of events detected from multiple electrodes suggested that synchronous discharges were often initiated from several subicular sites.

The mean frequency of synchronous events in slices was 1.2 ± 0.6 Hz ($n = 18$), close to that of interictal spikes detected from scalp (1.1 ± 0.3 Hz; $n = 14$) or depth EEG records (1.3 ± 0.4 Hz; $n = 4$) made from the same patients (Fig. 2, A and B). When identically filtered (bandpass, 1 to 100 Hz), events from in vitro records and intracranial EEG events were similar, consisting of a fast, negative spike followed by a slower, positive deflection (Fig. 2C). Their durations, from onset to peak positivity, were comparable (33 ± 11 ms, $n = 18$ slices; 65 ± 30 ms, $n = 4$ intracranial records). Discharges generated by subicular slices are thus comparable to interictal activity.

We examined the role of signaling by glutamate and γ -aminobutyric acid (GABA) in generation of this activity by using antagonists of excitatory and inhibitory amino acid receptors (17). Synchronous discharges were reversibly suppressed (Fig. 3A) by applying 2,3-dihydroxy-6-nitro-7-sulfamoylbenzo(f) quinoxaline (NBQX) and D,L-2-amino-5-

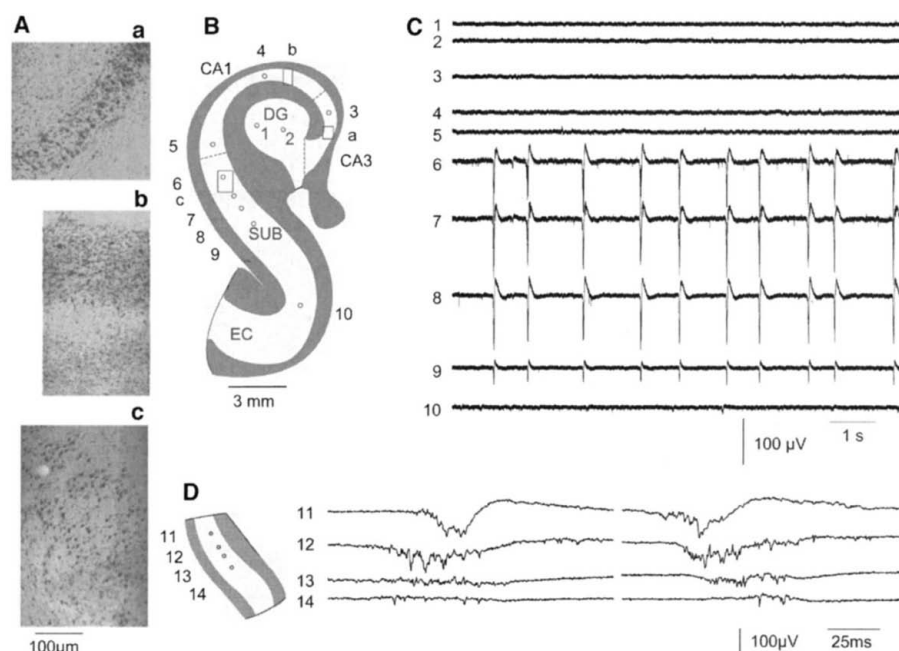


Fig. 1. Synchronous rhythmic activity is generated in the subiculum of human temporal lobe slices. (A) Sclerotic cell loss was evident in cresyl violet-stained sections of the CA3 (a) and CA1 (b) regions but less pronounced in the subiculum (c). (B) Diagram of a typical slice with gray areas corresponding to fibers. Rectangles labeled a to c indicate positions of photomicrographs in (A). (C) Spontaneous events were never observed from the CA3 and CA1 regions or the dentate gyrus (DG) (positions 1 to 5). Interictal-like activity was evident in records from the subiculum (SUB) (positions 6 to 9) but disappeared again toward the entorhinal cortex (EC) (position 10). (D) Records from isolated slices confirmed that the subiculum generates the interictal-like activity. Two events from the same slice showed variability in generation and propagation of synchronous events. Recording positions throughout correspond to numbers on inset diagrams.

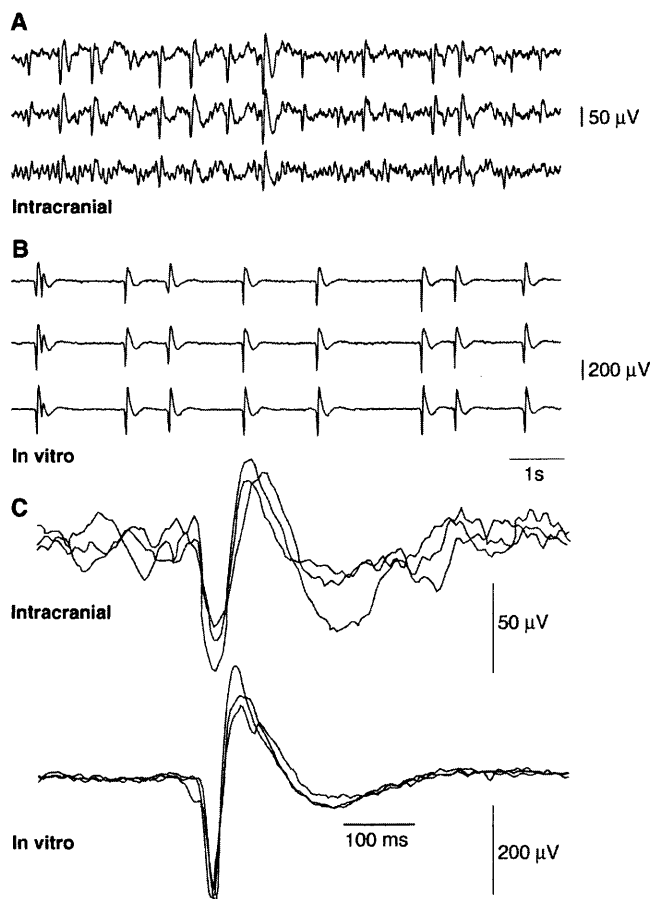


Fig. 2. In vitro interictal-like events resemble intracranial EEG records. (A) Synchronous spike and wave interictal events recorded from three intracranial EEG electrodes located in the mesial temporal lobe of a patient. (B) A slice from the same patient generates spontaneous events of similar frequency and shape (filtered as the EEG; 1 to 100 Hz). (C) Comparison of three superimposed events from in vitro and intracranial records reveals a similar form with a somewhat greater amplitude variability and longer duration for the intracranial interictal events.

REPORTS

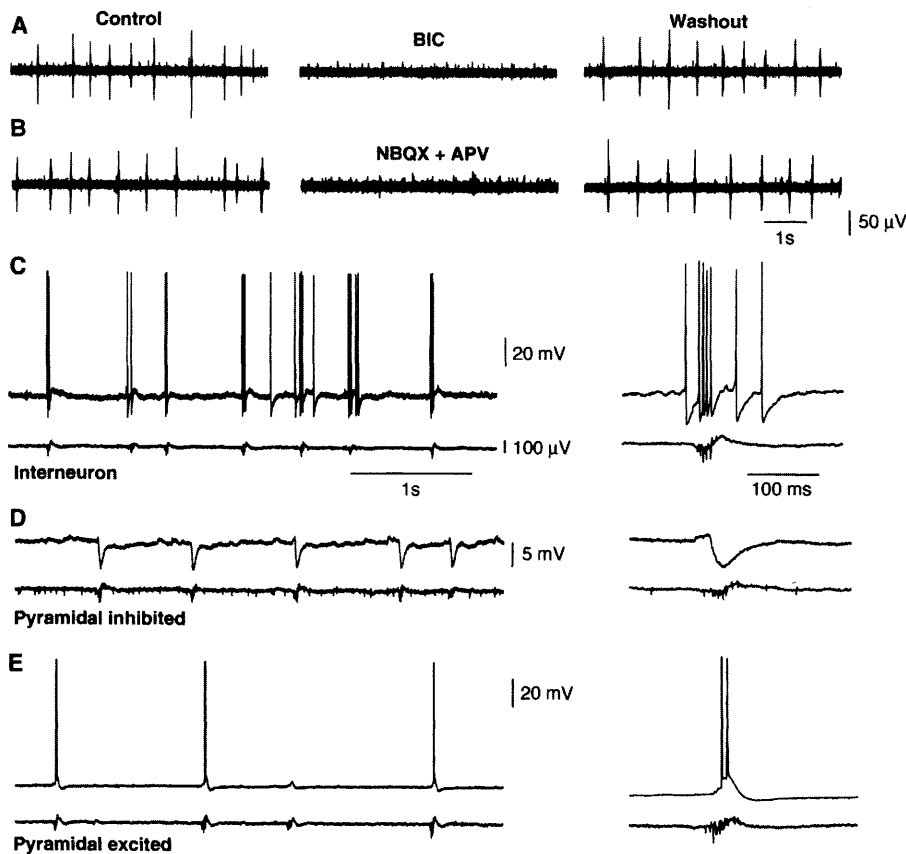


Fig. 3. Excitatory and inhibitory synaptic signaling both contribute to spontaneous interictal-like events. Spontaneous events were blocked by NBQX and APV, antagonists at glutamate receptors (A) and suppressed by the GABA_A receptor antagonist bicuculline (BIC) (B). (C to E) Different responses of subicular cells associated with interictal-like synchrony. Traces include intracellular records above and extracellular records below. (C) An interneuron was excited during the bursts. (D) A pyramidal cell received a small synaptic excitation followed by a larger inhibitory potential. (E) A pyramidal cell was excited and discharged simultaneously with interictal-like events.

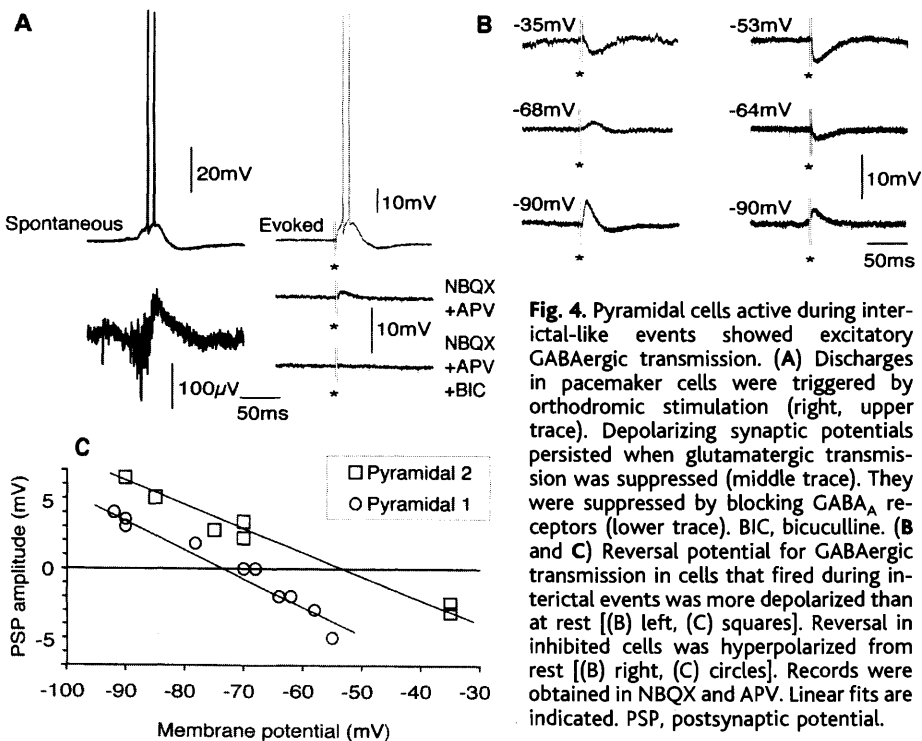


Fig. 4. Pyramidal cells active during interictal-like events showed excitatory GABAergic transmission. (A) Discharges in pacemaker cells were triggered by orthodromic stimulation (right, upper trace). Depolarizing synaptic potentials persisted when glutamatergic transmission was suppressed (middle trace). They were suppressed by blocking GABA_A receptors (lower trace). BIC, bicuculline. (B and C) Reversal potential for GABAergic transmission in cells that fired during interictal events was more depolarized than at rest [(B) left, (C) squares]. Reversal in inhibited cells was hyperpolarized from rest [(B) right, (C) circles]. Records were obtained in NBQX and APV. Linear fits are indicated. PSP, postsynaptic potential.

phosphovaleric acid (APV) ($n = 8$) or 6-cyano-7-nitroquinoxaline-2,3-dione (CNQX) and APV ($n = 8$). Surprisingly, these events were also blocked (Fig. 3B) by the GABA_A receptor antagonists bicuculline ($n = 3$), picrotoxin ($n = 2$), and gabazine ($n = 5$).

We made intracellular records ($n = 133$) to explore how both inhibitory and excitatory signaling were involved (Fig. 3, C to E). The mean resting potential of subicular cells was -62 ± 10 mV, mean input resistance was 35 ± 9 M Ω , and action potentials were overshooting. Human subicular neurons discharged action potentials repetitively or in bursts, as do pyramidal cells of rodent subiculum (18, 19). Interneurons ($n = 9$) were distinguished from pyramidal cells ($n = 124$) by distinct discharge patterns analogous to those of rodent hippocampus (18–20).

Inhibitory cells discharged before and during interictal population bursts (Fig. 3C). Pyramidal cells displayed different behaviors during synchronous events (Fig. 3, D and E). At resting potential, large, inhibitory synaptic potentials, sometimes preceded by small excitatory synaptic potentials, were detected in 78% ($n = 97$) of these neurons (Fig. 3D). In contrast, in a subgroup of 22% of pyramidal cells (Fig. 3E; $n = 27$) interictal-like bursts were associated with synaptic events that were excitatory at rest. These cells fired before and during interictal events and presumably, together with the interneurons, act as pacemaker cells in generating interictal synchrony.

The observation that inhibitory cells and a subgroup of pyramidal cells discharge during interictal-like bursts conforms to pharmacological data suggesting that both inhibitory and excitatory signaling contribute to this rhythmic activity. Potentially, the existence in subicular slices of a central, rhythmically active focus and an inhibited surround might explain the variability in pyramidal cell behavior (2, 21). However, in a single slice, pacemaker cells were not spatially segregated from those that were inhibited during population events.

We compared synaptic events initiated in the different types of pyramidal cells by activating afferent fibers. Extracellular stimuli triggered interictal-like discharges, which initiated firing in pacemaker cells (Fig. 4A; $n = 14$) and large inhibitory postsynaptic potentials (IPSPs) in inhibited cells (22). In pacemaker cells, blocking glutamatergic excitation with NBQX and APV ($n = 10$) did not reveal hyperpolarizing events. In four cells, the remaining synaptic potential reversed near resting potential. In the other six cells, the synaptic event was depolarizing and was blocked by GABA_A antagonists (Fig. 4A). This depolarizing GABAergic signaling in pacemaker cells, similar to that of early development (23), presumably contributes to rhythm generation.

GABAergic signaling is depolarizing (24)

when the reversal potential for ions passing through GABA receptor channels is more positive than resting potential. Therefore, we compared, in pacemaker and inhibited cells, resting potential and the reversal potential of synaptic events remaining in the presence of glutamate receptor blockers (Fig. 4, B and C). In pacemaker cells that discharged synchronously with interictal bursts, synaptic events recorded in NBQX and APV reversed at -55 ± 12 mV ($n = 9$), more depolarized ($P < 0.025$; Student's t test) than their resting potential of -67 ± 10 mV ($n = 9$). Synaptic events in inhibited cells, reversed at -72 ± 7 mV ($n = 25$), while the resting potential, -62 ± 8 mV ($n = 25$), was less hyperpolarized ($P < 0.001$). These data show that IPSPs reverse at potentials positive to rest (24, 25) in a subset of subicular neurons.

This *in vitro* activity corresponds in several respects to interictal activity in mesial temporal lobe epilepsy. Epileptiform bursts were generated in the subiculum but not in other regions, which suggests that they did not result from general defects in slice condition. Interictal activity seems to be generated by a minority of subicular neurons including interneurons and a subset of pyramidal cells (Fig. 3, C and E). Both glutamatergic and GABAergic signaling are involved (Fig. 3, A and B), in line with previous suggestions from work on epileptic human tissue (8). Reciprocal interactions between the three cell types may underlie the generation of this activity. The difference between discharging and inhibited pyramidal cells apparently results from different reversal potentials for GABAergic events. GABA-mediated synaptic events may also depolarize interneurons, although we did not test this explicitly.

One feature of the sclerotic hippocampus is the formation of aberrant connections between dentate granule cells (26, 27). Our data suggest that plastic changes also occur in the subiculum. Thus, loss of both postsynaptic (dentate gyrus to CA3) and presynaptic (CA1 to subiculum) cells initiates an epileptogenic plasticity. In the subiculum, the reactive plasticity includes changes in GABAergic signaling. A hyperexcitability in the subiculum would, unlike in the dentate region, permit propagation to other cortical structures. Our observation of depolarizing synaptic GABA responses in some subicular pyramidal cells recalls the GABAergic excitation of early development, which results from delayed expression of the KCC2 transporter (23, 24). Deafferentation may initiate a regressive switch in GABAergic response polarity from hyperpolarizing to depolarizing (25), perhaps in the most severely denervated cells. Understanding changes in the subiculum (4, 25) induced by the loss of excitatory inputs from CA1 cells may eventually provide therapeutic avenues for preventing seizure development after hippocampal insults.

References and Notes

1. D. V. Lewis, *Curr. Opin. Neurol.* **12**, 197 (1999).
2. M. Dichter, W. A. Spencer, *J. Neurophysiol.* **32**, 649 (1969).
3. R. K. S. Wong, R. D. Traub, *J. Neurophysiol.* **49**, 442 (1983).
4. R. A. McKinney *et al.*, *Nature Med.* **3**, 990 (1997).
5. P. Salin *et al.*, *J. Neurosci.* **15**, 8234 (1995).
6. R. S. Fisher, *Brain Res. Rev.* **14**, 245 (1989).
7. B. W. Colder *et al.*, *J. Neurophysiol.* **75**, 2496 (1996).
8. R. Kohling *et al.*, *Brain* **121**, 1073 (1998).
9. P. A. Schwartzkroin *et al.*, *Ann. Neurol.* **13**, 249 (1983).
10. P. A. Schwartzkroin, M. M. Haglund, *Epilepsia* **27**, 523 (1986).
11. Patients were between 22 and 54 years old and had suffered from pharmacoresistant focal seizures for 25 years on average. Seizure frequency was 11 ± 10 (mean \pm SD) per month. Functional imaging, morphological studies, and inspection of slices revealed a hippocampal sclerosis of variable severity. Surface EEG recordings were obtained from all patients, and intracranial recordings were obtained from hippocampal structures in four cases.
12. S. Lehericy *et al.*, *Neuroradiology* **39**, 788 (1997).
13. J. Engel Jr., *Curr. Opin. Neurol.* **7**, 140 (1994).
14. Portions of mesial temporal lobe, obtained from the neurosurgeon, with the patients' informed consent, were immediately immersed in 26 mM NaHCO₃, 1 mM KCl, 10 mM MgCl₂, 1 mM CaCl₂, 248 mM sucrose, and 10 mM glucose equilibrated with 5% CO₂ in 95% O₂ at 4°C. Hippocampal-subicular slices 400 μ m thick were prepared with a vibratome in the same solution and transferred to a recording chamber. They were maintained at 35° to 37°C, perfused with 124 mM NaCl, 26 mM NaHCO₃, 4 mM KCl, 2 mM MgCl₂, 2 mM CaCl₂, and 10 mM glucose and equilibrated with 5% CO₂ in 95% O₂. The time between tissue reception and slice preparation was typically 45 min.
15. Intracellular records were made with 2 M KAc-filled glass microelectrodes and extracellular signals were recorded with etched tungsten wires as described in [I. Cohen, R. Miles, *J. Physiol. (London)* **524**, 485 (2000)].
16. F. H. Lopes da Silva, M. P. Witter, P. H. Boeijinga, A. H. Lohman, *Physiol. Rev.* **70**, 453 (1990).
17. Fast excitatory postsynaptic potentials were blocked with 5 μ M NBQX or 20 μ M CNQX and 100 μ M APV. GABA_A receptor-mediated IPSPs were suppressed by picrotoxin (50 μ M), bicuculline (10 μ M), or gabazine (SR-95531; 5 μ M).
18. J. R. Greene, S. Totterdell, *J. Comp. Neurol.* **380**, 395 (1997).
19. M. Stewart, R. K. S. Wong, *J. Neurophysiol.* **70**, 232 (1993).
20. P. Parra, A. I. Gulyas, R. Miles, *Neuron* **20**, 983 (1998).
21. D. A. Prince, B. J. Wilder, *Arch. Neurol.* **16**, 194 (1967).
22. I. Cohen *et al.*, unpublished data ($n = 49$).
23. Y. Ben-Ari, E. Cherubini, R. Corradetti, J. L. Gaiarsa, *J. Physiol. (London)* **416**, 303 (1989).
24. C. Rivera *et al.*, *Nature* **397**, 251 (1999).
25. C. Vale, D. H. Sanes, *J. Neurosci.* **20**, 1912 (2000).
26. T. Sutula *et al.*, *J. Comp. Neurol.* **390**, 578 (1998).
27. P. R. Patrylo, F. E. Dudek, *J. Neurophysiol.* **79**, 418 (1998).
28. We thank P. Parra, D. Fricker, R. Traub, H. Korn, and F. Gabbiani for help and comments on the manuscript. Supported by INSERM, Fondation Française pour la Recherche sur L'Epilepsie, NIH (MH54671), CNRS, and Fondation pour la Recherche Médicale.

24 July 2002; accepted 4 October 2002

Transition State Stabilization by a Catalytic RNA

Peter B. Rupert,¹ Archana P. Massey,² Snorri Th. Sigurdsson,² Adrian R. Ferré-D'Amaré^{1*}

The hairpin ribozyme catalyzes sequence-specific cleavage of RNA through transesterification of the scissile phosphate. Vanadate has previously been used as a transition state mimic of protein enzymes that catalyze the same reaction. Comparison of the 2.2 angstrom resolution structure of a vanadate-hairpin ribozyme complex with structures of precursor and product complexes reveals a rigid active site that makes more hydrogen bonds to the transition state than to the precursor or product. Because of the paucity of RNA functional groups capable of general acid-base or electrostatic catalysis, transition state stabilization is likely to be an important catalytic strategy for ribozymes.

The hairpin ribozyme catalyzes reversible, site-specific cleavage of the phosphodiester backbone of RNA through transesterification (1) (Fig. 1A). The ribozyme is fully active *in vitro* when the physiologic counterion Mg²⁺ is replaced with cobalt (III) hexammine (2–4). This complex ion mimics hydrated Mg²⁺ but cannot directly coordinate or activate water or RNA ligands. Therefore, nucleic acid

moieties alone must be responsible for promoting cleavage 10⁶ times faster than the background rate.

A crystal structure of a hairpin ribozyme bound to an inhibitor RNA has been reported (5). The minor grooves of two irregular helices, stems A and B, dock to form the active site. One of the strands of stem A contains the scissile phosphate (Fig. 1B). In the crystal structure, the nucleotides flanking this phosphate are splayed apart (Fig. 1C), aligning the 2'-OH nucleophile (blocked with a methyl group to prevent cleavage) with the reactive phosphorus and the 5'-oxo leaving group. The in-line conformation (required for the second-order nucleophilic substitution transesterification) and biochemical and biophys-

¹Division of Basic Sciences, Fred Hutchinson Cancer Research Center, 1100 Fairview Avenue North, Seattle, WA 98109–1024, USA. ²Department of Chemistry, University of Washington, Box 351700, Seattle, WA 98195–1700, USA.

*To whom correspondence should be addressed. E-mail: afferre@fhcrc.org